Cardiovascular Research (2014) **104**, 258–269
doi:10.1093/cvr/cvu205

Study familial hypertrophic cardiomyopathy using patient-specific induced pluripotent stem cells

Lu Han[1], Yang Li[1], Jason Tchao[1], Aaron D. Kaplan[2], Bo Lin[1], You Li[1], Jocelyn Mich-Basso[1], Agnieszka Lis[2], Narmeen Hassan[1], Barry London[3], Glenna C.L. Bett[4], Kimimasa Tobita[1], Randall L. Rasmusson[2], and Lei Yang[1]*

[1]Department of Developmental Biology, University of Pittsburgh School of Medicine, 8117 Rangos Research Center, 530 45th Street, Pittsburgh, PA 15201, USA; [2]Center for Cellular and Systems Electrophysiology, Department of Physiology and Biophysics, SUNY, Buffalo, NY 14214, USA; [3]Department of Internal Medicine, Carver College of Medicine, University of Iowa, Iowa City, IA 52242, USA; and [4]Department of Obstetrics and Gynecology, SUNY, Buffalo, NY 14214, USA

Received 12 September 2013; revised 25 August 2014; accepted 3 September 2014; online publish-ahead-of-print 10 September 2014

Time for primary review: 41 days

Aims Familial hypertrophic cardiomyopathy (HCM) is one the most common heart disorders, with gene mutations in the cardiac sarcomere. Studying HCM with patient-specific induced pluripotent stem-cell (iPSC)-derived cardiomyocytes (CMs) would benefit the understanding of HCM mechanism, as well as the development of personalized therapeutic strategies.

Methods and results To investigate the molecular mechanism underlying the abnormal CM functions in HCM, we derived iPSCs from an HCM patient with a single missense mutation (Arginine442Glycine) in the MYH7 gene. CMs were next enriched from HCM and healthy iPSCs, followed with whole transcriptome sequencing and pathway enrichment analysis. A widespread increase of genes responsible for 'Cell Proliferation' was observed in HCM iPSC-CMs when compared with control iPSC-CMs. Additionally, HCM iPSC-CMs exhibited disorganized sarcomeres and electrophysiological irregularities. Furthermore, disease phenotypes of HCM iPSC-CMs were attenuated with pharmaceutical treatments.

Conclusion Overall, this study explored the possible patient-specific and mutation-specific disease mechanism of HCM, and demonstrates the potential of using HCM iPSC-CMs for future development of therapeutic strategies. Additionally, the whole methodology established in this study could be utilized to study mechanisms of other human-inherited heart diseases.

Keywords Induced pluripotent stem cells • Hypertrophic cardiomyopathy • Cardiomyocyte • Heart

1. Introduction

Familial hypertrophic cardiomyopathy (HCM) is a primary disorder of cardiac muscle, and is associated with thickened ventricular wall and ventricular septum, increased myocardial fibrosis, disorganized myofibres, and always accompanied with arrhythmic heart beatings.[1] It is the most common autosomal dominant cardiovascular disease, with a prevalence of 1:500.[1] The overall annual mortality rate of HCM is 1–5%.[2,3] It is also the most common cause of sudden cardiac death (SCD) in young people, and accounts for one-third of all SCD in competitive athletes.[2] Mutations in over 11 genes, most of which encode sarcomeric proteins have been identified in HCM patients.[3] Mutations in β-myosin heavy chain (β-MHC or MYH7) account for ∼45% of all identified HCM cases.[3] Although medications and surgery can partially improve symptoms, no specific treatments to prevent or to arrest the development of HCM are available. At the cellular level, HCM is characterized by the enlarged cardiomyocytes (CMs) with increased protein synthesis, re-activated fetal cardiac gene expression, disrupted contractility, and electrical remodelling.[3,4] Many HCM mutations seem to induce abnormal heart contractility by perturbing Ca^{2+} cycling, CM force generation, and/or adenosine triphosphate (ATP) hydrolysis.[2] HCM-associated arrhythmias are caused by the electrical remodelling in the heart.[4,5] Despite the progresses in HCM study, a remarkable deficit still exists in the understanding of the molecular mechanism, which leads from sarcomeric mutations to the diverse HCM disease phenotypes.

Currently, most mechanistic studies of HCM have been conducted in model systems, including transgenic and gene-targeted mice.[2] The difficulty to obtain heart tissues from healthy and HCM human hearts is the major obstacle for studying HCM using human cells. Recent advances in induced pluripotent stem cells (iPSCs) circumvent

* Corresponding author. Tel: +1 412 692 9842; fax: +1 412 692 6184, Email: lyang@pitt.edu

this hurdle.[6] To date, single CMs have been derived from iPSCs of patients with Leopard Syndrome,[7] Long QT syndrome,[8,9] dilated cardiomyopathy (DCM),[10] and familial HCM[11] to model some aspects of disease phenotypes *in vitro*. However, the genome-wide study of disease mechanisms using CMs derived from patient-specific iPSCs remains unknown due to the difficulty of obtaining CMs from iPSC cultures with a high purity.

In this study, we sought to establish a whole method for modelling heart disorders and studying mechanisms of inherited human heart diseases by using HCM patient-derived iPSCs as an example. Our HCM iPSCs carry a single missense mutation (R442G) in the MYH7 gene. As expected, HCM iPSC-derived CMs exhibited enlarged size, disorganized sarcomere structures and arrhythmic beatings. Using our established method,[12,13] CMs were obtained from HCM and control iPSCs with a high purity (~90%), followed with whole transcriptome sequencing. A large number of genes responsible for 'Cell Proliferation' were increased in HCM iPSC-CMs compared with control iPSC-CMs. This revealed the possible molecular mechanism of HCM using patient-derived iPSCs. Additionally, HCM iPSC-CMs exhibited irregular Ca^{2+} handling and ion-channel functions. Furthermore, we found pharmaceutical reagents could prevent the developments of CM hypertrophy and electrical irregularities in HCM iPSC-CMs. Overall, this study established a new platform to study personalized mechanisms of inherited heart diseases by combining iPSC reprogramming, highly efficient CM generation, whole transcriptome sequencing, and electrophysiological analyses. It would benefit the future development of personalized therapies for human-inherited heart diseases.

2. Methods

2.1 Generation of HCM patient-specific iPSCs

Skin biopsy was collected from a 37-year-old female patient with diagnosed HCM through the IRB of B.L. at University of Pittsburgh Medical Center (UPMC). This study was approved by University of Pittsburgh ethics review board and conformed to the Declaration of Helsinki. Patient consent was obtained for the use of fibroblasts. Dermal fibroblasts were reprogrammed to generate iPSCs by using retrovirus carrying SOX2, KLF4, OCT4, and c-MYC, respectively, as previously described.[6]

2.2 Animals

All animal studies conformed to the principles of the National Institutes of Health *Guide for the Care and Use of Laboratory Animals* (NIH publication no. 85–23, revised 1996), and Institutional Animal Care and Use Committee approved all protocols. Non-obese diabetic/severe combined immune deficiency (NOD/SCID) mice were anaesthetized in a chamber with the introduction of 100% CO_2 for 7–10 min. Euthanasia was accomplished by cervical dislocation.

2.3 Teratoma formation

It was conducted as a service in the transgenic core of Magee Women's Hospital, UPMC. 1×10^6 undifferentiated iPSCs were suspended in 10 μL Matrigel (BD Biosciences) and injected to the subrenal capsule of 8-week-old SCID/NOD mice. Eight weeks after cell delivery, tumours were explanted for haematoxylin and eosin staining.

2.4 Human iPSC culture and cardiac differentiation

Two healthy control iPSC lines were used here. The human S3-iPS4 has been previously generated[7] and the human Y1 iPSCs was established from healthy fibroblasts as previously described.[13] Both control iPSCs have been fully characterized.[7,13] The control and HCM iPSCs were maintained on MEFs with regular human embryonic stem-cell medium containing 10 ng/mL bFGF. iPSCs were differentiated into CMs using our previously established protocol.[12,13] The EBs were dissociated at around Day 24, seeded into 6-well plates and cultured as monolayers for additional 5 days. The drug treatments were performed with the CM monolayers. All growth factors were from R&D systems.

2.5 Whole-exome sequencing of patient-specific iPSCs

Genomic DNA was extracted from two clones of HCM iPSC clones for whole-exome sequencing. Details are available in the Supplementary material online.

2.6 Calcium imaging

The contractile CMs were incubated with media containing a Ca^{2+} indicator (Rhod-2 AM). Intracellular Ca^{2+} transients (CaiT) were optically recorded with a high spatiotemporal resolution CMOS camera as previously described.[13]

2.7 Whole transcriptome sequencing and data analysis

The whole transcriptomes of control S3-iPS4 and HCM iPSC-CMs C12 and C17 were sequenced and functional pathway enrichment was analysed using Ingenuity Pathway Analysis (IPA). (http://www.ingenuity.com/products/pathways_ analysis. html).[14] See Supplementary material online for details.

2.8 Quantitative PCR analysis

Real-time quantitative PCR (q-PCR) was performed on a 7900HT Fast Real-Time PCR System (Applied Biosystems) with Fast SYBR Green Master Mix (Applied Biosystems). Results were analysed with EXCEL, normalized to Cyclophinin G (CYPG) gene expression. Primer sequences are described in Supplementary material online, *Table S1*.

2.9 Electrophysiological recordings

Cardiac action potentials and ionic currents were recorded from iPSC-derived single CMs. See Supplementary material online for details.

2.10 Microelectrode array recording

iPSC-derived beating EBs were dissociated and seeded onto multi-electrode chambers to form synchronized monolayers for recording field potential duration (FPD), beating frequency (beats per minute, BPM) and interspike intervals (ISI). Signals were acquired with a MED64 amplifier (Multi Channel Systems) and digitalized by MC_rack and MC_datatool.

2.11 Data analysis

Electrophysiological data were analysed using pClamp 9 (Axon Instruments). Data are shown as means ± SD of three independent experiments. Statistical analysis was performed with Student's unpaired *t*-test and ANOVA. Two-tailed $P < 0.05$ was considered to be statistically significant.

3. Results

3.1 HCM iPSC reprogramming and genotyping

From the University of Pittsburgh Medical Center, we obtained skin biopsy from a 37-year-old female with diagnosed cardiac hypertrophy. Fibroblasts were grown out from the skin sample, followed with retroviral infection of four reprogramming factors OCT4, SOX2, KLF4, and c-MYC.[6] Four iPSC clones were established (*Figure 1A*). Next we conducted whole genomic DNA deep-sequencing of HCM iPSCs to identify

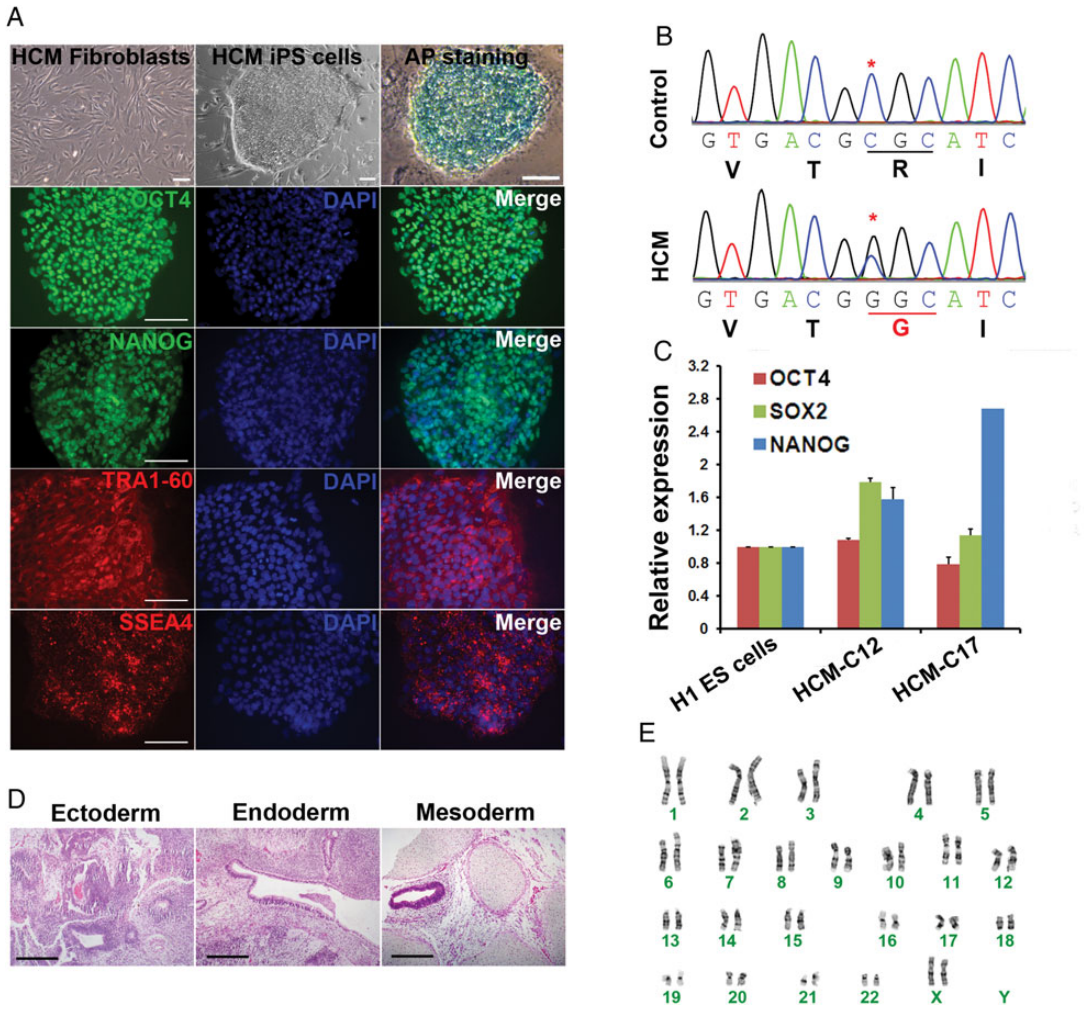

Figure 1 Establishment and characterization of HCM iPSCs. (*A*) Reprogramming of HCM dermal fibroblasts to iPSCs showing pluripotent stem cell morphology with positive AP staining and expression of pluripotency markers, OCT4, NANOG, TRA1-60, and SSEA4. Scale bars, 100 μm. (*B*) Sanger sequencing to confirm the R442G heterozygous missense mutation in the MYH7 gene from HCM patient-derived iPSCs. (*C*) Quantitative real-time PCR analysis of human ES cell line H1 and HCM iPSC clone12 and clone17 for detecting the expression of pluripotency marker genes OCT4, SOX2, and NANOG ($n = 3$). (*D*) Teratoma formation with HCM iPSCs showing three embryonic germ layers. Scale bar, 50 μm. (*E*) Karyotyping of HCM iPSCs.

disease-causing gene variants using the SOLiD™ Sequencing System (Life Technologies). Our whole-exome data were analysed by filtering coding variants against dbSNP138, 1000Genomes, and NHLBI EVS Exome databases. Full list of novel coding variants (<0.8% MAF in databases mentioned) are provided (Supplementary material online, *Table S2*). We noted that MYH7 C1324G was the only mutation present in genes known to cause HCM and this specific mutation has been previously identified to cause HCM in patients.[15] This C1324G mutation results in an Arginine to Glycine substitution at the amino acid position 442 (R442G) of MYH 7 protein and was confirmed using Sanger sequencing (*Figure 1B*). Pluripotency of HCM iPSCs was validated by immunostaining of OCT4, NANOG, TRA-1-60, and SSEA4, AP (AP) live staining (*Figure 1A*), q-PCR detection of NANOG, SOX2, OCT4 expressions in HCM iPSCs (*Figure 1C*), and the teratoma formation assay with *in vivo* generation of three germ layers (*Figure 1D*). A stable chromosomal integrity (46, XX) was revealed by karyotyping (*Figure 1E*). As previously described,[6] the diminishment of retroviral transgenes was detected in HCM iPSCs (Supplementary material online, *Figure S1A*). Taken together, all these data reveal the successful generation of HCM patient-specific iPSCs.

3.2 CM differentiation and genome-wide transcriptional profiling

In this study, two healthy human iPSC lines S3-iPS4 and Y-1 were used as normal controls. Both of them were generated and fully characterized as previously described.[7,13] Both control and HCM iPSCs were differentiated into CMs using our established method[13] (Supplementary material online, *Video S1*), which was modified from our previous cardiac differentiation protocol with human embryonic stem cells.[12] This protocol has been previously utilized for modelling Leopard Syndrome (LS)-associated HCM, DCM, and familial HCM with patient-derived iPSCs.[7,10,11] In this study, we screened multiple HCM iPSC clones and found two clones (HCM C12 and C17) could give rise to CMs with a high purity (*Figure 2A*). Thus CMs were obtained from HCM and control S3-iPS4 iPSCs, followed by whole transcriptome sequencing

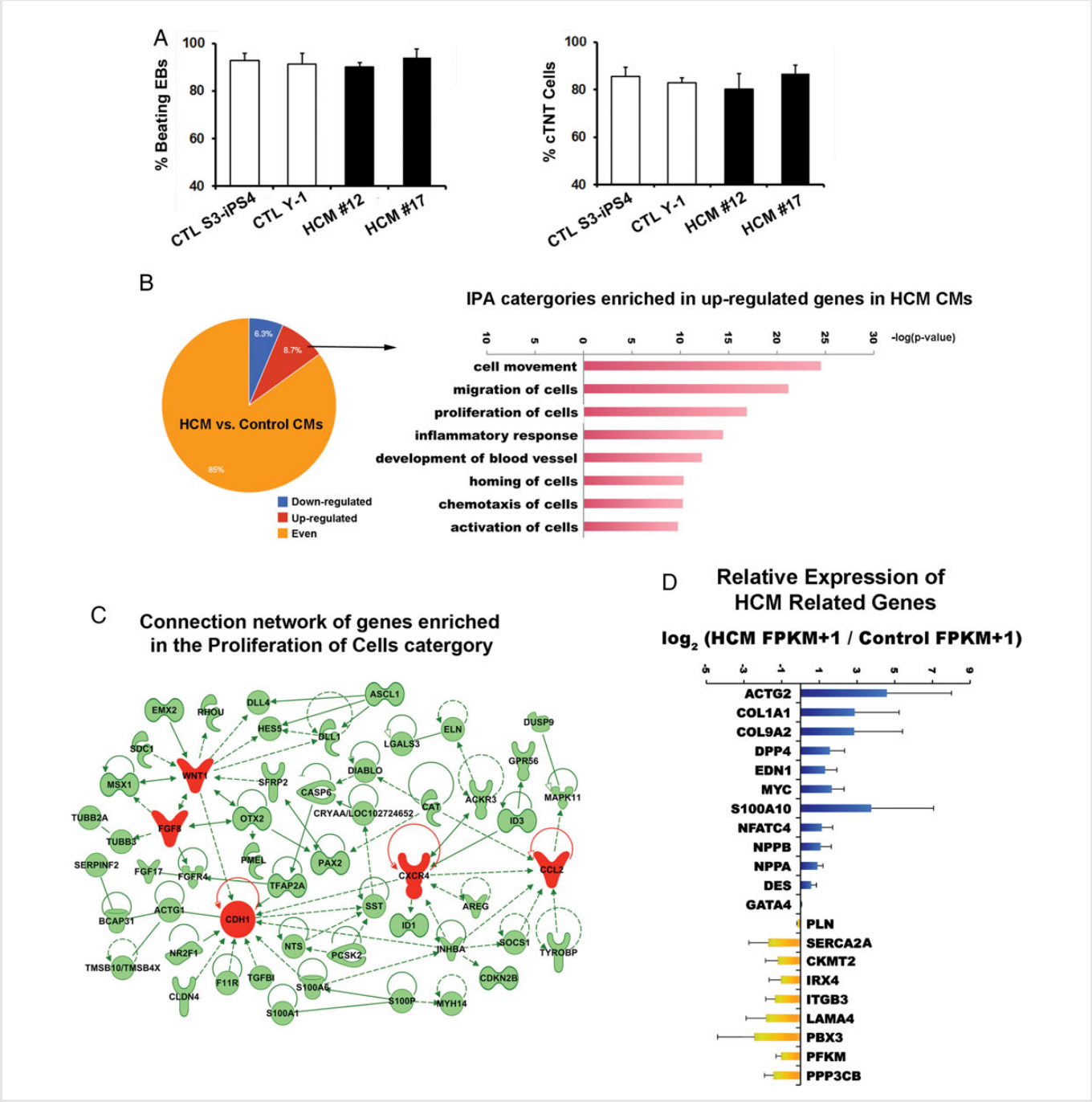

Figure 2 CM differentiation and gene expression profile of HCM iPSC-CMs. (*A*) The ratios of beating embryoid bodies ($n = 4$ for each line) at Day 22 of iPSC differentiation and ratios of CMs derived from day 22 EBs of control and HCM iPSCs. Cardiac Troponin T (CTNT) is a marker for CMs. (*B*) CMs derived from control S3-iPS4 and two clones of HCM iPSCs were used for whole transcriptome sequencing with an Ion Torrent Sequencer (Life Technologies). FPKMs from CMs of two HCM clones and control iPSCs ($n = 3$, each sample) were averaged and compared, which revealed both up-regulated and down-regulated genes in HCM iPSC-CMs (left panel). Ingenuity IPA bio-functional enrichment analysis was conducted with the up-regulated genes in HCM CMs, with the top enriched bio-functional categories shown in right panel. (*C*) The connection network of genes enriched in the Proliferation of Cells category. (*D*) Expression fold changes of HCM-related genes in HCM iPSC-CMs vs. control iPSC-CMs from Y1 and S3 iPSCs. Fold changes were represented as mean $\pm$ S.D in a $\log_2$ form.

using an Ion Torrent Sequencer (Life Technologies). In order to minimize the possible differences from HCM iPSC clones, CMs generated from the two iPSC clones were utilized for sequencing. The CM gene expressions from two HCM iPSC clones were then averaged and compared with that from the control iPSCs. Approximately 15% (~2000 genes) of all sequenced genes exhibited significant expression changes (>2-folds) in HCM iPSC-CMs vs. control iPSC-CMs (*Figure 2B*).[14] Next, we examined the biofunctional enrichment of differentially expressed genes by using IPA (Ingenuity Systems Pathway Analysis Software). Interestingly, the up-regulated genes in HCM CMs vs. control CMs were mostly associated with 'Cell Proliferation and Movement' bio-functional categories (*Figure 2B*). The sequencing results from CMs of

two HCM iPSC clones were very consistent (Supplementary material online, *Table S3*). This indicated that this group of genes, which regulate cell proliferation in HCM iPSC-CMs, might play an essential role in the developing of HCM. Therefore, we next utilized IPA to establish a functional gene connection network with all the up-regulated genes enriched in the IPA 'Proliferation of cells' category (*Figure 2C*) (Supplementary material online, *Table S3*). Interestingly, several genes, including WNT1, CDH1, CXCR4, FGF8, and CCL2 were found to be central regulators in this network, implying their critical role during the developing of human HCM. Previous studies indicated that the canonical Wnt/β-Catenin pathway could regulate cell proliferation in the early stage of heart development.[16,17] Additionally, activation of non-canonical Wnt pathway stimulates calcium release within CMs and in turn triggers the Calcineurin-NFAT signalling pathway, which is essential for activating cardiac growth and remodelling genes during cardiac hypertrophy.[18] Consistent with this observation, we found an increased level of nuclear NFATC4 in HCM iPSC-CMs when compared with control iPSC-CMs via immunostaining (*Figure 3A* and *C*). Besides WNT signalling pathway, the expression levels of FGF8 and FGF receptor-FGFR4 were increased in HCM iPSC-CMs. FGF signalling has been previously shown to regulate myocytes proliferation,[19–21] as well as to induce hypertrophy of CMs.[22–24] Moreover, the critical roles of CDH1 and CXCR4 in cancer cell proliferation have been previously studied,[25,26] albeit unclear in cardiac hypertrophy. However, it has been reported that WNT signalling could interact with CDH1 and CXCR4 in urothelial cells and neural progenitors.[27,28] *Figure 2D* shows the relative levels of some differentially expressed genes in HCM vs. control CMs from the whole-transcriptional sequencing analysis, which include HCM-related genes EDN1, NFACT4, NPPA, and NPPB and fibrosis-related genes COL1A1 and COL9A2. This gene expression change pattern is highly consistent with previous HCM studies in other models[29] and was validated by q-PCR (Supplementary material online, *Figure S1B*). Altogether, this analysis for the first time sought to explore the personalized molecular mechanism of human HCM using patient-derived

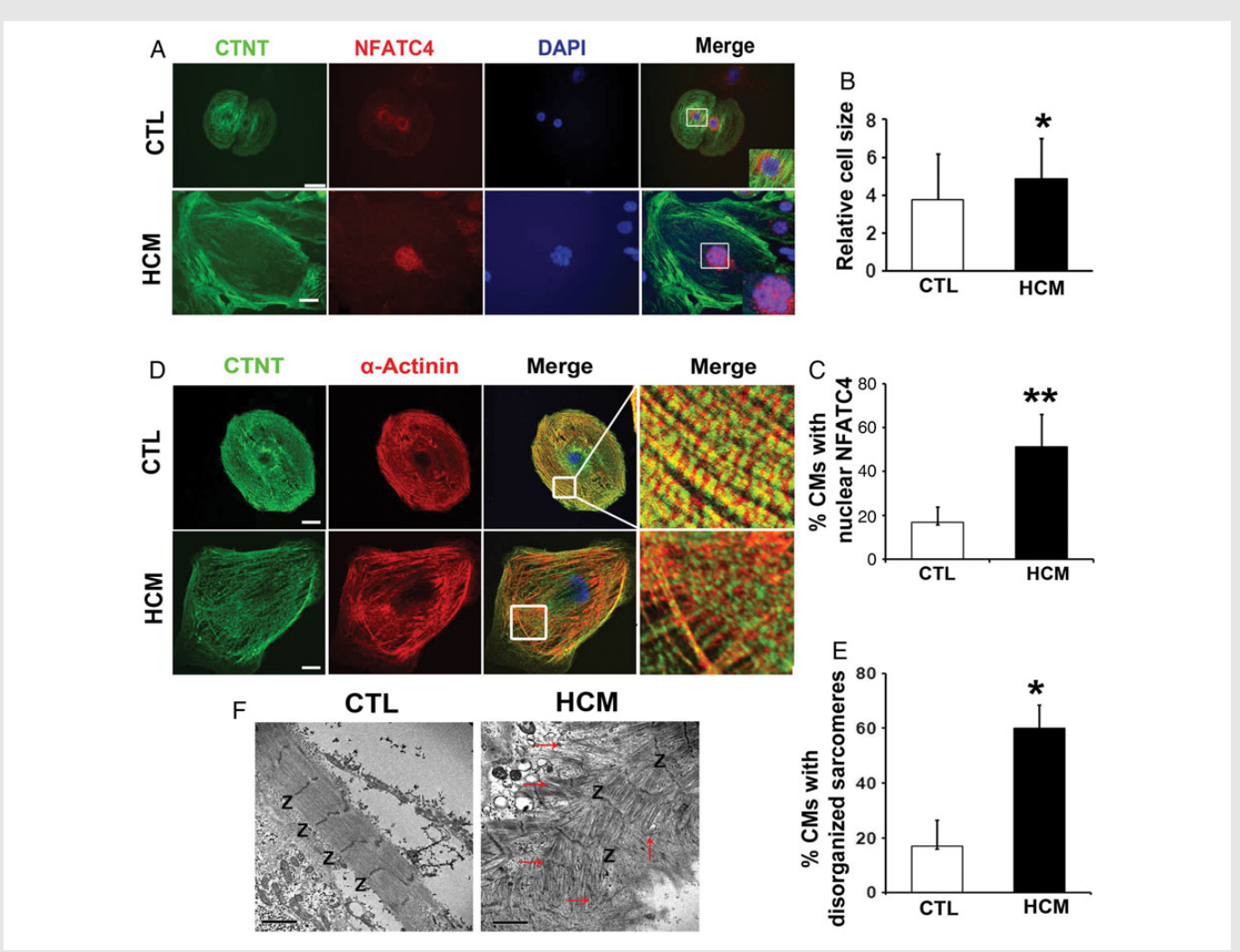

Figure 3 Phenotypic characterization of HCM iPSC-CMs. (*A*) Representative immunofluorescent images showing increased cell size and nuclear translocated NFATC4 in HCM iPSC-CMs. White frames indicated the multinucleation in HCM iPSC-CMs. Scale bars, 10 μm. (*B*) Quantification of CM size. $n = 105$. (*C*) Ratio of NFATC4 nuclear translocation in control and HCM iPSC-CMs. $n = 169$. (*D*) Representative immunostaining of CTNT and α-Actinin to show the sarcomere disorganization in HCM iPSC-CMs. Scale bars, 10 μm. (*E*) Ratio of sarcomere disorganization in control and HCM iPSC-CMs. $n = 150$. (*F*) Transmission Electron Microscopy images of myofibrillar organization in control and HCM iPSC-CMs. Scale bars, 500 nm. Z, Z band. Red arrows indicate the disorganized myofibrils. Error bars show SD. *$P < 0.05$, **$P < 0.01$. (Student's *t*-test).

iPSCs, indicating a cell-intrinsic mechanism to promote CM growth in this HCM patient.

3.3 Detecting sarcomere organization

At the cellular level, HCM is characterized by the enlarged CM size with disrupted contractility, implying the disorganized sarcomeres in HCM CMs.[1,2] First, CMs from control and HCM iPSCs were immunostained for a CM marker, Cardiac Troponin T (CTNT) (*Figure 3A*). Compared with the control, HCM iPSC-CMs exhibit a significantly larger surface area (*Figure 3B*) and an increased ratio of nuclear located NFATC4 (51.35 vs. 16.95%, $n = 169$) (*Figure 3A* and *C*). These results indicate a hypertrophic phenotype in HCM iPSC-CMs as previously described.[7] Next, Confocal microscopy detected an increased ratio of disrupted sarcomeres in HCM iPSC-CMs vs. control iPSC-CMs (42 vs.17%, $n = 150$) (*Figure 3D* and *E*). Lastly, using transmission electron microscopy (TEM), well-organized myofibrils with clearly defined Z bands were observed in the control iPSC-CMs, whereas the perturbed myofibrils with disorganized Z lines were found in the HCM iPSC-CMs (*Figure 3F*, Supplementary material online, *Figure S2*). All these results demonstrate the disrupted sarcomere organizations in HCM iPSC-CMs, implying mechanical abnormalities in HCM myocardium.

3.4 Electrophysiological behaviour of single HCM iPSC-CMs

HCM is generally associated with susceptibility to ventricular arrhythmia, multiple electrophysiological abnormalities, and heart failure.[1,5,30] Therefore, we first examined action potentials of single CM ventricular-like properties using whole cell patch clamp. The intracellular recording revealed a marked increase in action potential duration (APD) prolongation (*Figure 4A* and Supplementary material online, *Figure 3A*), and an increase in the degree of variability in HCM iPSC-CMs compared with control iPSC-CMs (CTL, $n = 23$; HCM, $n = 41$) (*Figure 4B*). The average APDs at 90% repolarization (APD90) and 50% repolarization (APD50) of spontaneous beating HCM iPSC-CMs were significantly longer than those of control iPSC-CMs (APD 90: 560.5 ± 81.3 vs. 910.4 ± 86.9 ms and APD50: 429.3 ± 84.1 vs. 756.4 ± 82.2 ms) (*Figure 4C*) and suggested a change in action potential shape to a less triangular shape in HCM iPSC-CMs vs. control iPSC-CMs (*Figure 4A*). Similar results were observed with the electrically stimulated, as opposed to spontaneously fired, HCM and control iPSC-CMs (Supplementary material online, *Figure S3A* and *B*). Interestingly, the change of APDs was also accompanied by changes in action potentials shape. While many action potentials had the characteristic rounded shape of the control cells (*Figure 4A*, CTL), there were 4 out of 25 CMs in the HCM group displaying an extremely exaggerated notch response (*Figure 4A*, HCM left) in morphology, which was not seen in matched controls or human HCM iPSC-CMs from a recent report.[4,11]

3.5 Electrophysiological behaviour of CM monolayers

Next, we sought to evaluate the electrophysiological properties from the multicellular level. Microelectrode array (MEA) was used to measure the field potentials of CM clusters (Supplementary material online, *Figure S4A*, *B* and *Video S2*).[9] The extracellular recording exhibited prolonged and dispersed interspike intervals (ISI) in HCM iPSC-CMs compared with control iPSC-CMs (*Figure 4D*). The recording of irregular potentials in HCM iPSC-CMs (*Figure 4D* and *E*, Supplementary material online, *Figure S4C* and *D*) led to increased arrhythmogenic events (19% in HCM vs. 4% in control, *Figure 4F*). Lastly, an increased irregular contractility was detected from synchronized HCM iPSC-CM monolayers using the Real-Time Cell Analyzer (RTCA, Roche) (*Figure 4G* and *H*, Supplementary material online, *Figure S5* and *Video S3*). All these indicate the electrophysiological abnormalities of HCM iPSC-CMs.

3.6 Calcium transient behaviour in HCM iPSC-CMs

Myocyte excitation–contraction coupling is stringently regulated, in part, through the modulation of calcium (Ca^{2+}) influx release and removal sequestration.[31] Calcium influx through L-type calcium channels and calcium release from sarcoplasmic reticulum (SR) contribute importantly to APD formation and have a key role in arrhythmia.[32] We analysed Ca^{2+} handling in HCM and control iPSC-CMs using optical mapping. Compared with control CMs, HCM CMs exhibited a significant irregularity of calcium transient (*Figure 5A* and *B*). The resting level of Ca^{2+} ($[Ca^{2+}]_i$) was significantly elevated in HCM CMs compared with control CMs (21% increase, $n = 51$) (*Figure 5C* and *D*). In the heart, Ca^{2+} enters the myocytes through the voltage-gated L-type Ca^{2+} channels, which in turn triggers Ca^{2+}-mediated Ca^{2+} release from the sarcoplasmic reticulum (SR) by the ryanodine receptor (RYR2). During diastole, Ca^{2+} reuptake into the SR is mediated by the SR Ca^{2+} -ATPase (SERCA). Therefore, we measured the SR Ca^{2+} storage with caffeine treatment, which induces the Ca^{2+} release from SR into cytoplasm. HCM CMs exhibited a lower Ca^{2+} transient increase after caffeine administration, indicating a depressed Ca^{2+} storage in the SR of HCM CMs (*Figure 5E* and *F*), which could be due to the decreased level of RYR2 (Supplementary material online, *Figure S1B*). In addition, Ca^{2+} transient of HCM CMs exhibited a delayed decay time, indicating compromised diastole of HCM CMs (*Figure 5G*, $P = 2.05E\text{-}07$), which could be caused by the decreased SERCA2A expression in HCM CMs (*Figure 2D*) as previously observed.[33,34] Furthermore, we measured the voltage- gated L-type Ca^{2+} current. The HCM CMs showed a pronounced increase of Ca^{2+} currents compared with control CMs (*Figure 5H*, upper panel). Cav1.2, which is a major subunit of Ca^{2+} channel expressed in CMs,[35,36] showed an increased level in HCM CMs when compared with control CMs (*Figure 5H*, lower panel). Additionally, increased sodium and outward potassium currents were observed in HCM CMs than in control CMs (*Figure 5I* and *J*, Supplementary material online, *Figure S6*). Taken together, HCM iPSC-CMs exhibited altered ion channel and SR functions, consistent with previous HCM studies in animal and human cells.[11,30] These findings suggest that the abnormal calcium handling of HCM iPSC-CMs due to the single MYH7 mutation could play an essential role in the pathogenesis of HCM.

3.7 Pharmaceutical treatment of HCM CMs

HCM patient iPSC-CMs provide an *in vitro* model to evaluate therapeutic benefits of pharmaceutical agents. Both control and HCM iPSC-CMs were treated with a β-adrenergic agonist, isoproterenol, which is known to trigger cardiac hypertrophy and heart failure in animals.[37,38] Administration of 1 μM isoproterenol (Iso) for 5 days increased the beating frequencies of control and HCM CMs (*Figure 6A*), and significantly elevated premature beats and irregular beating rates in HCM CMs (*Figure 6A*, *D* and Supplementary material online, *Figure S5C* and *D*). We next tested the response of HCM CMs to several drug reagents, which are currently in clinical use for HCM therapy. First, β1-adrenergic blocker metoprolol (Meto, 10 μM) was added into HCM CMs post-isoproterenol treatment. Metoprolol significantly decreased beating

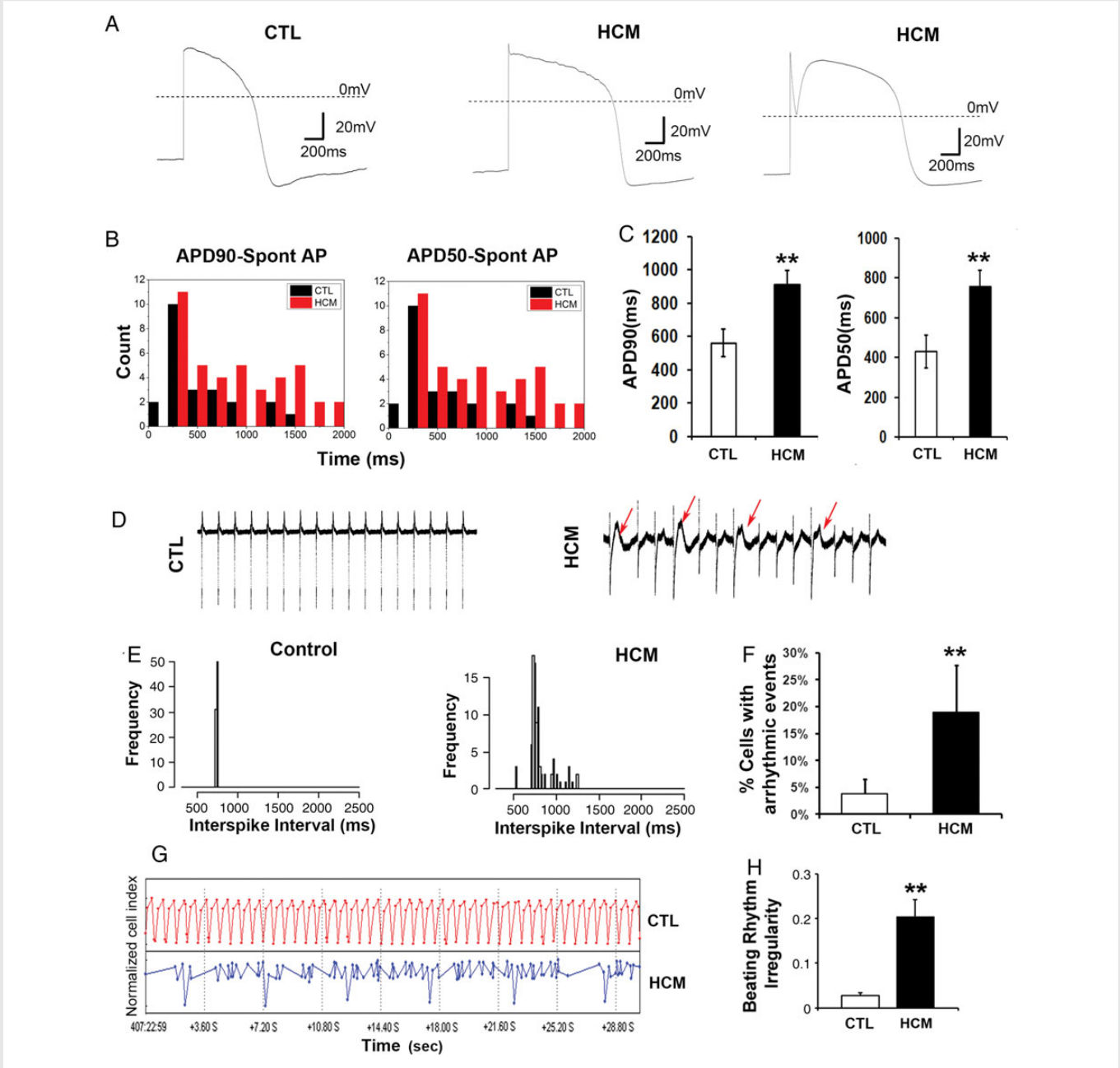

Figure 4 Electrophysiological analyses of HCM iPSC-CMs. (*A*) Representative action potential recordings from single control and HCM iPSC-CMs. (*B*) APD50 and APD90 distributions of spontaneously beating CMs. (CTL, $n = 23$; HCM, $n = 41$) (*C*) Quantification of APD50/90 of control and HCM iPSC-CMs. $^{**}P < 0.01$. (*D*) Representative MEA extracellular recording from control and HCM iPSC-CMs. HCM iPSC-CMs exhibit elevated arrhythmogenicity. Red arrows indicate the premature beats. (*E*) Interspike interval (ISI) distribution in control and HCM iPSC-CMs. (*F*) Quantification of arrhythmogenic events in control and HCM iPSC-CMs. $^{**}P < 0.01$. ($n = 12$) (Student's *t*-test). (*G*) Beating rhythm analysis of monolayer CMs using the RTCA system. Irregular beating pattern was observed from the HCM iPSC-CMs. (*H*) Quantification of beating rhythm irregularity during a period of 10 h. Data were collected for every 10 min ($n = 10$). Error bars show SD. $^{**}P < 0.01$. (Student's *t*-test).

irregularity and reduced arrhythmia in HCM CMs (*Figure 6B, C* and *E*). Because Ca^{2+} influx through L-type Ca^{2+} channel contributes importantly to arrhythmia induction,[31,39] we next applied a Ca^{2+} channel blocker, verapamil (100 nM), to HCM CMs post-metoprolol treatment. This continuous treatment with verapamil for additional 4 days completely eliminated irregular beats in HCM CMs (*Figure 6B, C* and *E*). Verapamil treatment ameliorated calcium handling abnormalities and depressed beating rhythm irregularity in HCM CMs, probably through decreasing the resting Ca^{2+} level and shortening Ca^{2+} transient duration (Supplementary material online, *Figure S4E–G*). In addition, long-term treatment of verapamil with high concentrations (>250 nM) could induce the cessation of spontaneous beating in iPSC-CMs (data not shown), indicating the feasibility of using human iPSC-CMs for drug safety testing. Lastly, we continuously treated HCM CMs with pinacidil (1 μM) post verapamil. Pinacidil is a K_{ATP} channel opener and clinically used as an antihypertensive drug. However, it induced irregular interspike intervals in the HCM CMs (*Figure 6C*). These results revealed a personalized response of HCM iPSC-CMs to drug reagents and indicate the

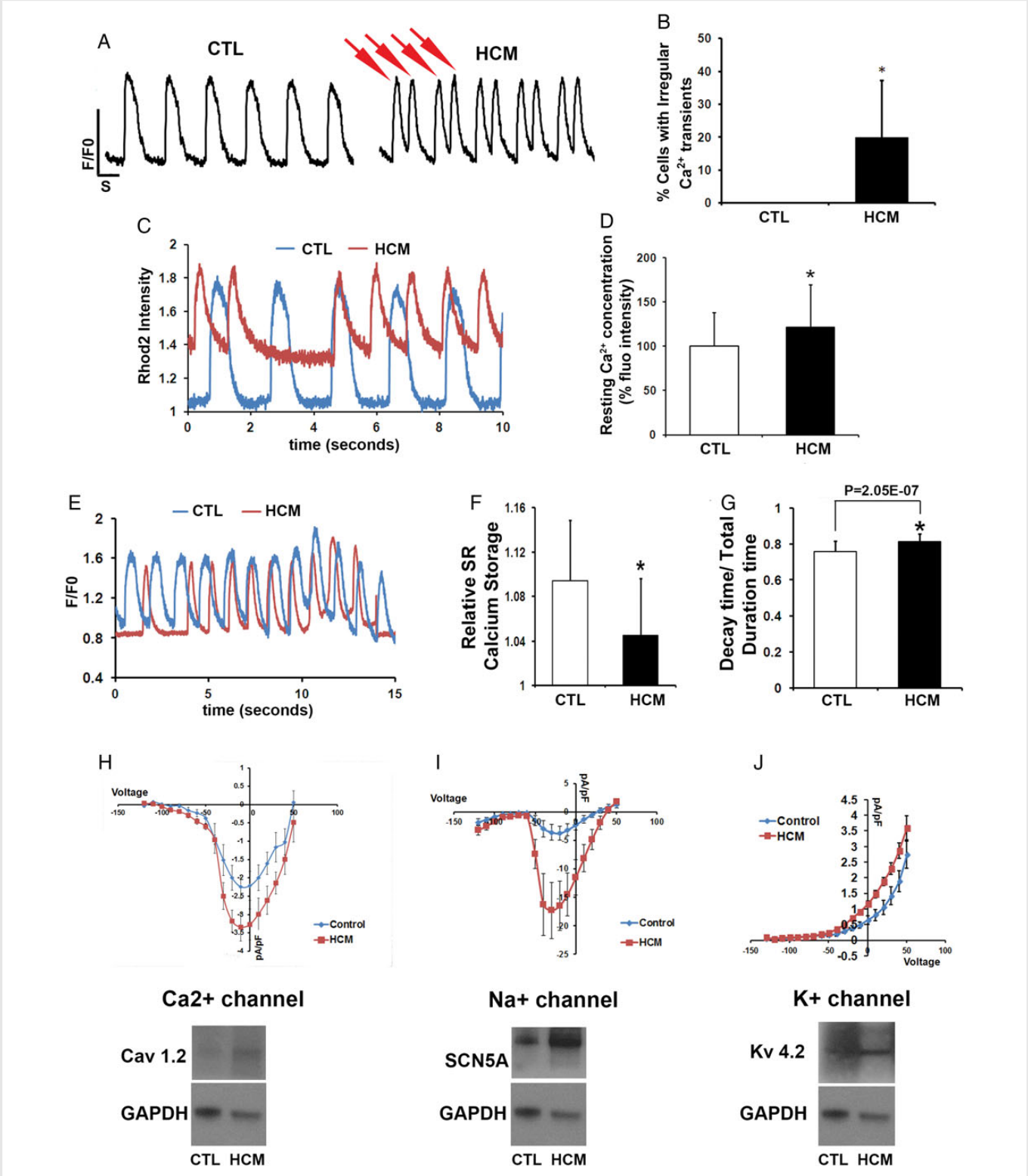

Figure 5 Analysis of calcium handling and ion channels. (*A*) Representative calcium transient optical mapping indicating irregular calcium transients in HCM iPSC-CMs (Red arrows). (*B*) Quantification of calcium irregularity in control and HCM iPSC-CMs ($n = 30$). (*C*) Representative calcium transient mapping showing elevated resting $[Ca^{2+}]_i$ in HCM CMs. (*D*) Quantification of resting $[Ca^{2+}]_i$ in control and HCM CMs ($n = 51$). (*E*) Representative image of calcium release in control and HCM CMs post caffeine (5 mM) treatment. (*F*) Quantification of relative Ca^{2+} storage in SR ($n = 11$ control, $n = 9$ HCM). (*G*) Quantification of calcium transient decay time in control and HCM CMs. ($n = 48$ control, $n = 50$ HCM, $P = 2.05E\text{-}07$). (*H*) Measurement of I_{Ca} followed depolarizing potentials of −130 to 50 mV in 10 mV increments ($n = 6$) and western blot of Cav1.2 in control and HCM CMs. (*I*) Measurement of Na^+ current magnitudes followed depolarizing potentials of −130 to 50 mV in 10 mV increments ($n = 31$) and western blot of SCN5A in control and HCM CMs. (*J*) Measurement of outward K^+ currents followed depolarizing potentials of −130 to 50 mV in 10 mV increments ($n = 10$) and western blot of Kv4.2 in control and HCM CMs. Current-to-Voltage (I–V) relationships were normalized with respect to cell capacitance. Error bars show SD. *$P < 0.05$. (Student's *t*-test).

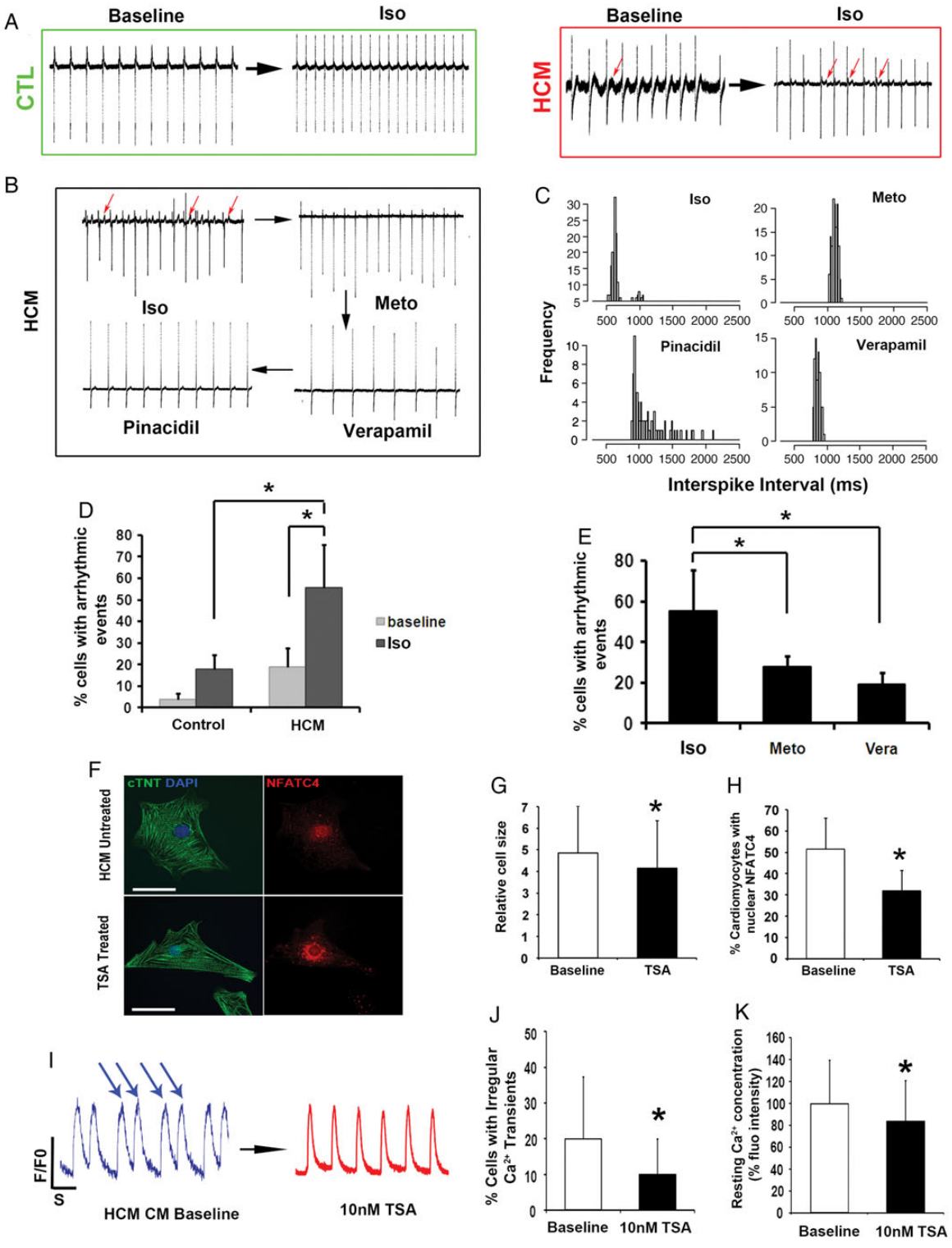

Figure 6 Pharmaceutical treatment of HCM iPSC-CMs. (*A*) Representative field potentials (MEA) of baseline and post-adrenergic agonist isopreterenol treatment from control and HCM iPSC-derived monolayer CMs. (*B*) Field potential trace of sequential drug treatments with isopreterenol, metoprolol, verapamil, and pinacidil in HCM iPSC-derived monolayer CMs by MEA. (*C*) Change of interspike interval of field potentials in HCM CMs after sequential drug treatments. (*D*) Quantification of arrhythmic events in control and HCM CMs after isopreterenol treatment ($n = 5$). (*E*) Quantification of arrhythmic events in HCM CMs with isopreterenol, metopronol, or verapamil treatment, respectively ($n = 5$) (ANOVA analysis). (*F*) Representative immunostaining images of HCM CMs without/with the treatment of 10 nM Trichostatin A (TSA) for 3 days. Scale bars, 20 μm. (*G*) Quantification of size change of HCM CM ($n = 77$). (*H*) Ratio of NFATC4 nuclear translocation in HCM CMs ($n = 164$). (*I*) Representative Ca^{2+} transient of HCM CMs with/without TSA (10 nM) treatment for 3 days. (*J*) Quantification of Ca^{2+} transient irregularity in HCM CMs ($n = 30$). (*K*) Quantification of resting Ca^{2+} in HCM CMs ($n = 30$). Error bars show SD. *$P < 0.05$. (Student's *t*-test).

significance of using patient-specific iPSC-CMs for developing personalized therapeutic strategies for human HCM.

Previous studies indicated that inhibition of histone deacetylase (HDAC) activity could prevent the progress of cardiac hypertrophy in animal and cellular HCM models.[40–42] However, the mechanism of HDACs in suppressing cardiac hypertrophy remains unclear. In this study, we tested whether Trichostatin A (TSA), which is a pan-inhibitor of histone deacetylases, could prevent the development of disease phenotypes in HCM iPSC-CMs. Remarkably, continuous administration of TSA (10 nM) for 3 days significantly ameliorated various hypertrophic phenotypes of HCM CMs, including the decreased CM size (*Figure 6F* and *G*, $n = 83$, $P < 0.05$) and suppressed NFATC nuclear translocation (*Figure 6F* and *H*. 51.35 vs. 31.93%, $n = 169$, $P < 0.05$). TSA also suppressed calcium irregularity (20 vs. 10%, *Figure 6I* and *J*) by decreasing the resting $[Ca^{2+}]_i$ (*Figure 6K*). Altogether, our results indicate that TSA could possibly prevent cellular hypertrophy through decreasing the cytosolic Ca^{2+} overload of the HCM iPSC-CMs, demonstrating the feasibility of using HCM iPSC-CMs for future evaluating and screening of therapeutic compounds.

4. Discussion

Human MYH7 gene contains 38 exons. Up to 45% of familial HCM individuals carry mutations in MYH7.[3] Over 1000 mutations have been identified to cause HCM and many are in the different functional domains of MYH7 protein, which may account for the phenotypic diversity in HCM patients. In addition, the same MYH7 mutation can result in a variable disease penetrance and phenotypic severity in patients. All these indicate that, beyond the MYH7 mutations, the patient-specific genetic backgrounds significantly contribute to the varying clinical symptoms. Currently, most mechanistic studies of HCM have been conducted in model systems, including transgenic and gene-targeted mice.[2] However, given the genetic heterogeneity of HCM patients, the limited HCM animal models could not represent the over 1000 mutations in HCM patients. Thus, the development of translational therapy of HCM, especially the personalized medicine, requires the uncovering of personalized disease mechanism as a first step.

Recently, CMs have been derived from iPSCs of patients with various inherited heart diseases,[7,9–11] and were utilized to model some aspects of disease phenotypes. However, the progress of disease modelling with iPSCs requires more personalized approaches, such as the genome-wide study of patient-specific disease mechanism. In this study, by conducting whole transcriptome-sequencing with CMs enriched from HCM and control iPSCs, we for the first time explored the patient-specific and mutation-specific HCM disease mechanism using patient-derived iPSCs. Our whole-transcriptional analysis suggested the possible important roles of several signalling pathways in the development of CM hypertrophy. In particular, we found WNT1 could be a central regulator of cell proliferation in human HCM iPSC-CMs, implying that WNT1 could be a potential therapeutic target of human HCM. Additionally, increased expression levels of Notch signalling pathway genes, such as DLL1/4 and FGF pathway genes, such as FGF8/FGFR4, were observed in HCM iPSC-CMs, indicating that multiple signalling pathways have been involved in the developing of HCM. Our next study is to conduct a comprehensive analysis of all differentially expressed genes in HCM vs. control iPSC-CMs, with a specific focus on genes enriched into multiple signalling pathways and the interactions of those signalling pathways, which could provide deeper insights into the molecular mechanism of HCM. Additionally, previous genotype–phenotype correlation studies have shown significant variability in the phenotype expression of HCM among affected individuals with identical disease-causing mutations, which suggest the possible existence of modifier genes that determine the disease phenotypic severities in HCM patients.[43] However, functional modifier genes in HCM largely remain unclear. It is our expectation that the technologies developed in this report, such as whole transcriptome sequencing and phenotypic assessments, together with the existing knowledge from large-scale genome-wide studies of HCM, could uncover and validate functional modifier genes in individual HCM patient.

Consistent with the previous report,[11] our HCM iPSC-CMs exhibited enlarged cellular size, disrupted sarcomere structures, and disorganized CM myofibrils, indicating the compromised contraction machinery in HCM iPSC-CMs. In addition, we observed an abnormal Ca^{2+} handling in our HCM iPSC-CMs (Arg442Gly), which is similar to previous observations from HCM iPSC-CMs with a different MYH7 mutation (Arg663His).[11] The administration of verapamil could suppress the arrhythmic beats in both studies, indicating the imbalance of Ca^{2+} homeostasis is the major cause of arrhythmogenic events in MYH7 mutation-caused HCM. HCM iPSC-CMs (Arg442Gly) of this study did not exhibit an increased ratio of delayed afterdepolarizations (DAD), which was found in the previous Arg663His HCM iPSC-CMs.[11] However, we observed elongated APDs and exaggerated notch response in APD morphology in our HCM iPSC-CMs (Arg442Gly). All these differences suggest the possible impact of patient-specific genetic background on the disease phenotypic diversity, or the mutations on the different functional domains of MYH7 protein could lead to the differing electrophysiological irregularities. This is consistent with the previous observations that mutations within the head vs. tail domain of MYH7 could cause different levels of severities of cardiac hypertrophy and incidences of SCD in HCM patients.[44,45]

Our findings demonstrated a combined defect of L-type calcium influx and intracellular $[Ca^{2+}]_i$ handling in HCM iPSC-CMs (Arg442Gly), which might be caused by elevated expression of calcium channel protein Cav1.2. The HCM iPSC-CMs also exhibited the reduced function of calcium induced calcium release (CICR) from SR, which is consistent with the decreased expressions of RYR2 and SERCA2 in HCM iPSC-CMs. In addition, HCM iPSC-CMs showed pronounced increases of sodium, and outward potassium transient currents. Dysfunction in ion-channel homeostasis is the major trigger of cardiac arrhythmias, which is a serious complication in most HCM patients.[4,46] Thus, a major therapeutic target in HCM is to limit the development of life-threatening cardiac arrhythmia. Current medical management of HCM-associated arrhythmia, such as using β-blocker and calcium blocker, has remained unchanged over the past decades. We tested the response of our HCM iPSC-CMs to those anti-arrhythmia pharmaceutical reagents, and found reduced arrhythmia post drug administration. In addition, administration of TSA in our HCM iPSC-CMs eliminated irregular beatings and decreased the intracellular $[Ca^{2+}]_i$. Taken together, our results highlight the potential of iPSC-based technology for the future screening of pharmaceutical drugs to suppress HCM-associated arrhythmia.

Here we compared the disease phenotypes between HCM and two healthy control iPSC-CMs. Given the recent development of human genome-editing tools such as CRISPR,[47] it would be ideal as our next study to generate an isogenic control by correcting the MYH7 mutation in HCM iPSCs, which could be utilized to further confirm that abnormal CM phenotypes are caused by the specific MYH7 mutation. Some of our observations from HCM iPSC-CMs might not be exactly the same as

previous HCM studies, which aimed to summarize common disease phenotypes from all clinical HCM patients. For example, a recent study from Coppini *et al.*[4] analysed the electrophysiological properties of CMs isolated from 26 HCM patients with/without genetic mutations. The prolonged action potentials with increased late sodium and calcium currents were observed in that report, which are similar as our observations in this study. Opposite to our study, decreased repolarizing K^+ currents and no significant changes of Nav1.5 expressions were found from 10 of 26 HCM patients, which were claimed as representative phenotypic properties for all HCM patients in that report. However, due to the lack of genotyping information from those HCM patients, it is not clear whether such differences were due to the different patient backgrounds or varying HCM mutations. It is important to note that in the current report, we sought to examine the patient-specific and mutation-specific HCM disease phenotype and mechanism, whereas Coppini's paper sought to summarize common HCM phenotypes from a group of HCM patients with varying genetic backgrounds and mutations. Although some of our results look different, the difference lies in our different views from a single vs. a group of HCM patients.

Supplementary material

Supplementary material is available at *Cardiovascular Research* online.

Acknowledgements

We would like to acknowledge Dr. Ashok Srinivasan and Mr. Shanping Shi for excellent technical assistance.

Conflict of interest: none declared.

Funding

This work is supported by the University of Pittsburgh start-up, NIH UL1 TR000005 (University of Pittsburgh Clinical and Translational Science Institute, the Vascular Medicine Institute, the Hemophilia Center of Western Pennsylvania, and the Institute for Transfusion Medicine), and AHA SDG Grant (#11SDG5580002) to L.Y.; NIH R21 HL094402 and COMMONWEALTH OF PA (4100061184) to K.T.; NIH T32-HL76124 to J.T.; AHA GIA and NIH HL062465 to R.L.R.; National Heart and Lung Institute, HL093631 to G.C.L.B. Funding to pay the Open Access publication charges for this article was provided by University of Pittsburgh Start-up to L.Y.

References

1. Maron BJ. Hypertrophic cardiomyopathy: a systematic review. *JAMA* 2002;**287**:1308–1320.
2. Ahmad F, Seidman JG, Seidman CE. The genetic basis for cardiac remodeling. *Annu Rev Genomics Hum Genet* 2005;**6**:185–216.
3. Maron BJ, Maron MS, Semsarian C. Genetics of hypertrophic cardiomyopathy after 20 years: clinical perspectives. *J Am Coll Cardiol* 2012;**60**:705–715.
4. Coppini R, Ferrantini C, Yao L, Fan P, Del Lungo M, Stillitano F, Sartiani L, Tosi B, Suffredini S, Tesi C, Yacoub M, Olivotto I, Belardinelli L, Poggesi C, Cerbai E, Mugelli A. Late sodium current inhibition reverses electromechanical dysfunction in human hypertrophic cardiomyopathy. *Circulation* 2013;**127**:575–584.
5. Tomaselli GF, Marban E. Electrophysiological remodeling in hypertrophy and heart failure. *Cardiovasc Res* 1999;**42**:270–283.
6. Takahashi K, Tanabe K, Ohnuki M, Narita M, Ichisaka T, Tomoda K, Yamanaka S. Induction of pluripotent stem cells from adult human fibroblasts by defined factors. *Cell* 2007;**131**:861–872.
7. Carvajal-Vergara X, Sevilla A, D'Souza SL, Ang YS, Schaniel C, Lee DF, Yang L, Kaplan AD, Adler ED, Rozov R, Ge Y, Cohen N, Edelmann LJ, Chang B, Waghray A, Su J, Pardo S, Lichtenbelt KD, Tartaglia M, Gelb BD, Lemischka IR. Patient-specific induced pluripotent stem-cell-derived models of leopard syndrome. *Nature* 2010;**465**:808–812.
8. Moretti A, Bellin M, Welling A, Jung CB, Lam JT, Bott-Flugel L, Dorn T, Goedel A, Hohnke C, Hofmann F, Seyfarth M, Sinnecker D, Schomig A, Laugwitz KL. Patient-specific induced pluripotent stem-cell models for long-QT syndrome. *N Engl J Med* 2010;**363**:1397–1409.
9. Itzhaki I, Maizels L, Huber I, Zwi-Dantsis L, Caspi O, Winterstern A, Feldman O, Gepstein A, Arbel G, Hammerman H, Boulos M, Gepstein L. Modelling the long QT syndrome with induced pluripotent stem cells. *Nature* 2011;**471**:225–229.
10. Sun N, Yazawa M, Liu J, Han L, Sanchez-Freire V, Abilez OJ, Navarrete EG, Hu S, Wang L, Lee A, Pavlovic A, Lin S, Chen R, Hajjar RJ, Snyder MP, Dolmetsch RE, Butte MJ, Ashley EA, Longaker MT, Robbins RC, Wu JC. Patient-specific induced pluripotent stem cells as a model for familial dilated cardiomyopathy. *Sci Transl Med* 2012;**4**:130ra147.
11. Lan F, Lee AS, Liang P, Sanchez-Freire V, Nguyen PK, Wang L, Han L, Yen M, Wang Y, Sun N, Abilez OJ, Hu S, Ebert AD, Navarrete EG, Simmons CS, Wheeler M, Pruitt B, Lewis R, Yamaguchi Y, Ashley EA, Bers DM, Robbins RC, Longaker MT, Wu JC. Abnormal calcium handling properties underlie familial hypertrophic cardiomyopathy pathology in patient-specific induced pluripotent stem cells. *Cell Stem Cell* 2013;**12**:101–113.
12. Yang L, Soonpaa MH, Adler ED, Roepke TK, Kattman SJ, Kennedy M, Henckaerts E, Bonham K, Abbott GW, Linden RM, Field LJ, Keller GM. Human cardiovascular progenitor cells develop from a KDR+ embryonic-stem-cell-derived population. *Nature* 2008;**453**:524–528.
13. Lin B, Kim J, Li Y, Pan H, Carvajal-Vergara X, Salama G, Cheng T, Lo CW, Yang L. High-purity enrichment of functional cardiovascular cells from human iPS cells. *Cardiovasc Res* 2012;**95**:327–335.
14. Trapnell C, Roberts A, Goff L, Pertea G, Kim D, Kelley DR, Pimentel H, Salzberg SL, Rinn JL, Pachter L. Differential gene and transcript expression analysis of RNA-seq experiments with TopHat and Cufflinks. *Nat Protoc* 2012;**7**:562–578.
15. Laredo R, Monserrat L, Hermida-Prieto M, Fernandez X, Rodriguez I, Cazon L, Alvarino I, Dumont C, Pinon P, Peteiro J, Bouzas B, Castro-Beiras A. [Beta-myosin heavy-chain gene mutations in patients with hypertrophic cardiomyopathy]. *Rev Esp Cardiol* 2006;**59**:1008–1018.
16. Ueno S, Weidinger G, Osugi T, Kohn AD, Golob JL, Pabon L, Reinecke H, Moon RT, Murry CE. Biphasic role for Wnt/beta-catenin signaling in cardiac specification in zebrafish and embryonic stem cells. *Proc Natl Acad Sci USA* 2007;**104**:9685–9690.
17. Naito AT, Shiojima I, Akazawa H, Hidaka K, Morisaki T, Kikuchi A, Komuro I. Developmental stage-specific biphasic roles of Wnt/beta-catenin signaling in cardiomyogenesis and hematopoiesis. *Proc Natl Acad Sci USA* 2006;**103**:19812–19817.
18. Bergmann MW. Wnt signaling in adult cardiac hypertrophy and remodeling: lessons learned from cardiac development. *Circ Res* 2010;**107**:1198–1208.
19. Armstrong MT, Lee DY, Armstrong PB. Regulation of proliferation of the fetal myocardium. *Dev Dyn* 2000;**219**:226–236.
20. Pasumarthi KB, Kardami E, Cattini PA. High and low molecular weight fibroblast growth factor-2 increase proliferation of neonatal rat cardiac myocytes but have differential effects on binucleation and nuclear morphology. Evidence for both paracrine and intracrine actions of fibroblast growth factor-2. *Circ Res* 1996;**78**:126–136.
21. Lavine KJ, Yu K, White AC, Zhang X, Smith C, Partanen J, Ornitz DM. Endocardial and epicardial derived FGF signals regulate myocardial proliferation and differentiation in vivo. *Dev Cell* 2005;**8**:85–95.
22. Clarke MS, Caldwell RW, Chiao H, Miyake K, McNeil PL. Contraction-induced cell wounding and release of fibroblast growth factor in heart. *Circ Res* 1995;**76**:927–934.
23. Kaye D, Pimental D, Prasad S, Maki T, Berger HJ, McNeil PL, Smith TW, Kelly RA. Role of transiently altered sarcolemmal membrane permeability and basic fibroblast growth factor release in the hypertrophic response of adult rat ventricular myocytes to increased mechanical activity in vitro. *J Clin Invest* 1996;**97**:281–291.
24. Vatner SF. Fgf induces hypertrophy and angiogenesis in hibernating myocardium. *Circ Res* 2005;**96**:705–707.
25. Dong LL, Liu L, Ma CH, Li JS, Du C, Xu S, Han LH, Li L, Wang XW. E-cadherin promotes proliferation of human ovarian cancer cells in vitro via activating MEK/ERK pathway. *Acta Pharmacol Sin* 2012;**33**:817–822.
26. Shen B, Zheng MQ, Lu JW, Jiang Q, Wang TH, Huang XE. CXCL12-CXCR4 promotes proliferation and invasion of pancreatic cancer cells. *Asian Pacific J Cancer Prevent* 2013;**14**:5403–5408.
27. Luo Y, Cai J, Xue H, Mattson MP, Rao MS. SDF1alpha/CXCR4 signaling stimulates beta-catenin transcriptional activity in rat neural progenitors. *Neurosci Lett* 2006;**398**:291–295.
28. Thievessen I, Seifert HH, Swiatkowski S, Florl AR, Schulz WA. E-cadherin involved in inactivation of Wnt/beta-catenin signalling in urothelial carcinoma and normal urothelial cells. *Br J Cancer* 2003;**88**:1932–1938.
29. Friddle CJ, Koga T, Rubin EM, Bristow J. Expression profiling reveals distinct sets of genes altered during induction and regression of cardiac hypertrophy. *Proc Natl Acad Sci USA* 2000;**97**:6745–6750.
30. Frey N, Luedde M, Katus HA. Mechanisms of disease: hypertrophic cardiomyopathy. *Nat Rev Cardiol* 2011;**9**:91–100.
31. Bers DM. Calcium cycling and signaling in cardiac myocytes. *Annu Rev Physiol* 2008;**70**:23–49.
32. January CT, Riddle JM. Early afterdepolarizations: mechanism of induction and block. A role for l-type Ca^{2+} current. *Circ Res* 1989;**64**:977–990.
33. Schotten U, Koenigs B, Rueppel M, Schoendube F, Boknik P, Schmitz W, Hanrath P. Reduced myocardial sarcoplasmic reticulum Ca(2+)-atpase protein expression in compensated primary and secondary human cardiac hypertrophy. *J Mol Cell Cardiol* 1999;**31**:1483–1494.
34. Somura F, Izawa H, Iwase M, Takeichi Y, Ishiki R, Nishizawa T, Noda A, Nagata K, Yamada Y, Yokota M. Reduced myocardial sarcoplasmic reticulum Ca(2+)-atpase

mrna expression and biphasic force-frequency relations in patients with hypertrophic cardiomyopathy. *Circulation* 2001;**104**:658–663.
35. Catterall WA. Structure and regulation of voltage-gated Ca^{2+} channels. *Annu Rev Cell Dev Biol* 2000;**16**:521–555.
36. Keung EC. Calcium current is increased in isolated adult myocytes from hypertrophied rat myocardium. *Circ Res* 1989;**64**:753–763.
37. Fatkin D, Graham RM. Molecular mechanisms of inherited cardiomyopathies. *Physiol Rev* 2002;**82**:945–980.
38. Knollmann BC, Kirchhof P, Sirenko SG, Degen H, Greene AE, Schober T, Mackow JC, Fabritz L, Potter JD, Morad M. Familial hypertrophic cardiomyopathy-linked mutant troponin T causes stress-induced ventricular tachycardia and Ca^{2+}-dependent action potential remodeling. *Circ Res* 2003;**92**:428–436.
39. Molkentin JD, Lu JR, Antos CL, Markham B, Richardson J, Robbins J, Grant SR, Olson EN. A calcineurin-dependent transcriptional pathway for cardiac hypertrophy. *Cell* 1998;**93**:215–228.
40. McKinsey TA. The biology and therapeutic implications of hdacs in the heart. *Handb Exp Pharmacol* 2011;**206**:57–78.
41. McKinsey TA. Therapeutic potential for hdac inhibitors in the heart. *Annu Rev Pharmacol Toxicol* 2012;**52**:303–319.
42. Kee HJ, Kook H. Roles and targets of class I and IIa histone deacetylases in cardiac hypertrophy. *J Biomed Biotechnol* 2011;**2011**:928326.
43. Marian AJ. Modifier genes for hypertrophic cardiomyopathy. *Curr Opin Cardiol* 2002;**17**:242–252.
44. Marian AJ, Roberts R. The molecular genetic basis for hypertrophic cardiomyopathy. *J Mol Cell Cardiol* 2001;**33**:655–670.
45. Moore JR, Leinwand L, Warshaw DM. Understanding cardiomyopathy phenotypes based on the functional impact of mutations in the myosin motor. *Circ Res* 2012;**111**:375–385.
46. Semsarian C, Ahmad I, Giewat M, Georgakopoulos D, Schmitt JP, McConnell BK, Reiken S, Mende U, Marks AR, Kass DA, Seidman CE, Seidman JG. The L-type calcium channel inhibitor diltiazem prevents cardiomyopathy in a mouse model. *J Clin Invest* 2002;**109**:1013–1020.
47. Wiedenheft B, Sternberg SH, Doudna JA. Rna-guided genetic silencing systems in bacteria and archaea. *Nature* 2012;**482**:331–338.